CORONA INFLUENCE ON LIGHTNING INDUCED OVERVOLTAGES IN MOV-PROTECTED MULTICONDUCTOR POWER LINES

A. Andreotti[*], R. Araneo[**], S. Celozzi[**], L. Verolino[*]
[*] Dept. of Electrical Engineering, University of Naples *Federico II*, ITALY
[**] Dept. of Electrical Engineering, University of Rome "La Sapienza", ITALY

Abstract - The effects of corona on amplitude and distortion of lightning overvoltages in three-phase MV lines is investigated. The line is protected by surge-arresters whose characterstics can be planned taking into account real phenomena.

1. Introduction

Coupling of lightning electromagnetic field to transmission lines is a very well established research topic and literature is extremely broad. Despite this, the intrinsic dependance upon undetermined factors and uncertainties affecting some of the phenomena under examination call for deeper analyses and accurate models of real configurations.

In particular, the goal of this work is the evaluation of the influence of corona on three-phase medium voltage distribution lines protected by metal-oxyde surge arresters (MOV).

Corona has been simulated by means of two different approaches: the first one is based on the approximation of measured q-v curves, the second expresses analytically the voltage-dependence of the conductors radii, from which the dynamic capacitance matrix terms may be evaluated. In both cases it has been assumed that a delay, in the order of fractions of microsecond, occurs before the cause (voltage) yields to the corresponding effect (charge), after corona inception. Because of the distributed nonlinearities an FDTD algorithm has been adopted [1], allowing for an accurate simulation of the travelling waves attenuation and distortion.
The coupling mechanism in terms of both distributed voltage and current sources has been preferred to those in terms of scattered quantities. The lightning electromagnetic field is usually evaluated by considering the stroke channel as a vertical antenna above a ground plane [2-3]. Starting from the lightning current at the channel base [4], for the return stroke the MTL (Modified Transmission Line) model [5-7] to specify the space-time distribution of the current along the channel has been adopted, even though inaccuracies are known [5] to be inherent in the model, in some cases.

Ground losses have been shown to be important as concerns long lines [8] and the horizontal electric field component.

2. Lightning and distributed sources models

Several equivalent models have been proposed in the past to simulate the interaction of an external field with transmission lines [9-11]. In this work the formulation proposed by Taylor, Satterwhite and Harrison has been chosen, expressed in terms of total voltages and currents, because of the presence of distributed nonlinearities which require the knowledge of the total voltage at each position along the line. Thus, with reference to the configuration shown in Fig. 1, the following equation system has to be solved:

$$-\frac{\partial[V(t,x)]}{\partial x}=[L]\frac{\partial[I(t,x)]}{\partial t}-[e_{ds}(x,t)] \qquad (1a)$$

$$-\frac{\partial[I(t,x)]}{\partial x}=[C_{dyn}(v)]\frac{\partial[V(t,x)]}{\partial t}+[j_{ds}(t,x)] \qquad (1b)$$

where [V] and [I] are, respectively, the vectors of the line-to-ground voltages and line currents, [L] is the matrix of external inductances.

In (1) $[C_{dyn}]$ is the matrix of the dynamic capacitances accounting for the corona phenomenon, as described in

Section 3, and $[e_{ds}]$ and $[j_{ds}]$ are the vectors of the distributed voltage and current sources.

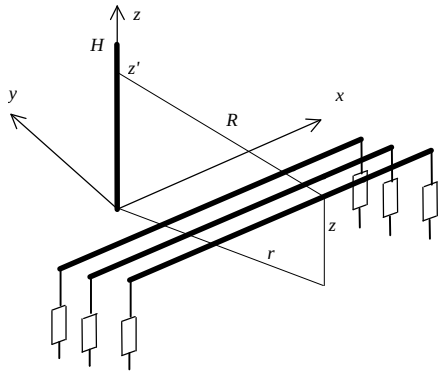

Figure 1 - Line configuration.

Ground losses have been neglected; their inclusion will introduce a convolution integral in the right hand side of (1a), accounting for the frequency-dependence of the p.u.l. impedance due to conductors and ground. Moreover, a finite value of the conductivity will affect the reflected field components and, thus, the distribued sources, also because of an additional term accounting for the horizontal electric field at the ground level [11]. In the following, the ground resistivity will be assumed to be zero, in this way overvoltages are estimated in excess.

2.1 Lightning model: the return stroke

The model used in the present analysis is the MTL, which takes into account the effects of propagation and damping along the lightning channel. The current at the time instant *t* and at the abscissa *z'* of the stroke channel is given by:

$$\mathrm{i}(\mathrm{z}',\mathrm{t}) = \mathrm{i}(0,\mathrm{t}-\mathrm{z}'/\mathrm{v})\exp(-\mathrm{z}'/\lambda)\mathrm{u}(\mathrm{t}-\mathrm{z}'/\mathrm{v}) \qquad (2)$$

where *v* is the velocity of the return-stroke, l is a decay constant and $u(t)$ is the step function. The expression for the channel base current $i(0,t)$ is the one proposed by Heidler [4]

$$i(0,t) = \frac{I_0}{h}\frac{(t/t_1)^n}{1+(t/t_1)^n}\exp(-t/t_2) \qquad (3)$$

where the amplitude correction factor h is

$$\eta = \exp\left[-(\tau_1/\tau_2)(n\tau_2/\tau_1)^{1/n}\right], \qquad (4)$$

and I_0 is the amplitude of the channel-base current, t_1 and t_2 are the front and decay time constants, n is an integer number between 2 and 10.

This model has been preferred to the double-exponential one, because it exhibits a null time-derivative at *t=0*, in accordance with the physical phenomenon. Additionally, it allows for the adjustment of the current amplitude, front and decay time almost independently by varying I_0, t_1, t_2, respectively. In this paper a sum of two functions (3) has been chosen in order to better reproduce the overall waveshape of the current observed in typical experimental results [2]. In Figure 2 the current $i(0,t)$ is plotted assuming, for the above parameters, the values reported in Table 1.

Table 1. Channel-base current parameters

I_{01} [kA]	t_{11} [ms]	t_{12} [ms]	n_1	I_{02} [kA]	t_{21} [ms]	t_{22} [ms]	n_2
10.7	0.25	2.5	2	6.5	2.1	230	2

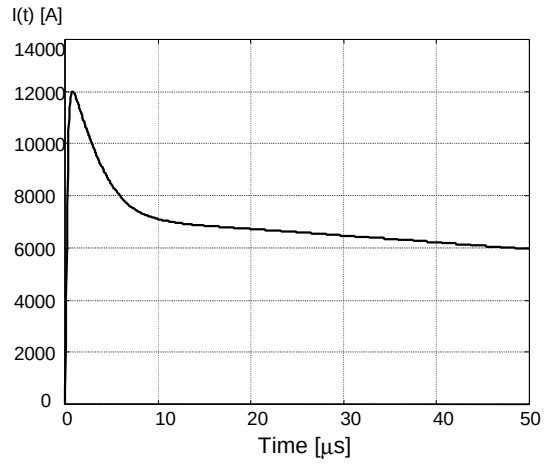

Figure 2 - Channel base current

2.2 Lightning electromagnetic field

In the calculation of the electromagnetic field associated to the lightning return stroke we will assume the ground as a perfect conductor. This is a reasonable approximation for the vertical component of the electric field and for the azimuthal component of the magnetic field [11] which are the components we will take into account to evaluate the distributed sources.

In the hypothesis of perfectly conducting ground, the vertical and the horizontal components of the electromagnetic field are given in [12]. In the time domain these expressions read

$$E_z(r,z,t)=\frac{1}{4\pi\varepsilon_0}\left[\int_{-H}^{H}\frac{2(z-z')^2-r^2}{R^5}\left(\int_0^t i(z',t-R/c)dt\right)dz'\right.$$

$$+\int_{-H}^{H}\frac{2(z-z')^2-r^2}{cR^4}i(z',t-R/c)dz'$$

$$\left.-\int_{-H}^{H}\frac{r^2}{c^2R^3}\frac{\partial i(z',t-R/c)}{\partial t}dz'\right] \qquad (5a)$$

$$B_j(r,z,t)=\frac{\mu_0}{4\pi}\left[\int_{-H}^{H}\frac{r}{R^3}i(z',t-R/c)dz'+\right.$$

$$\left.\int_{-H}^{H}\frac{r}{cR^2}\frac{\partial i(z',t-R/c)}{\partial t}dz'\right]. \qquad (5b)$$

2.3 Distributed sources

The distributed voltage and current sources in (1) can be expressed by simple integrals expressed in terms of the y-component of the magnetic flux density due to the lightning channel and the z-component of the electric field, both computed at the line position and in absence of the line itself:

$$[e_{ds}(t,x)]=\frac{\partial}{\partial t}\int_0^h B_y^i(t,x,z)dz \qquad (6a)$$

$$[j_{ds}(t,x)]=[C_{geo}]\frac{\partial}{\partial t}\int_0^h E_z^i(t,x,z)\,dz \qquad (6b)$$

As shown in Figs. 3 and 4, and generally accepted in literature, the vertical component of the electric field and the transverse magnetic flux density are practically constant along z and thus, integrations may be avoided.

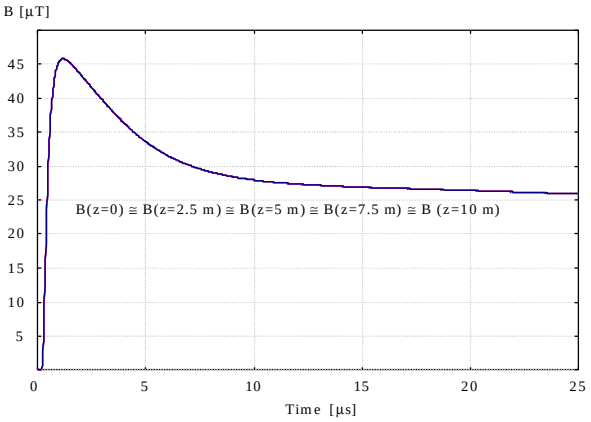

Figure 3 - Transverse magnetic flux density due to a lightning channel at 50 meters from the line, at different heights above the ground.

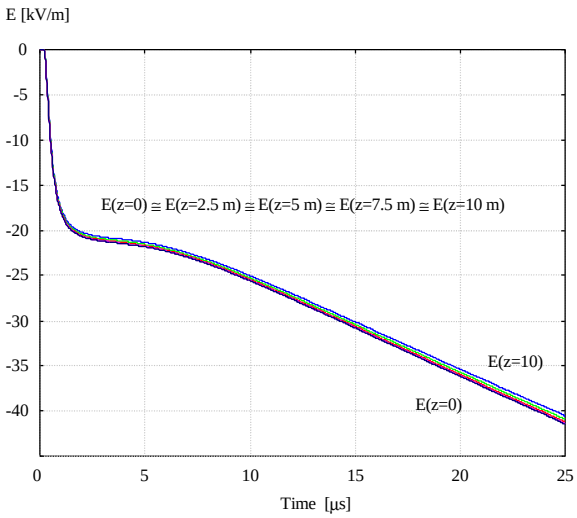

Figure 4 - Vertical electric field due to a lightning channel at 50 meters from the line, at different heights above the ground.

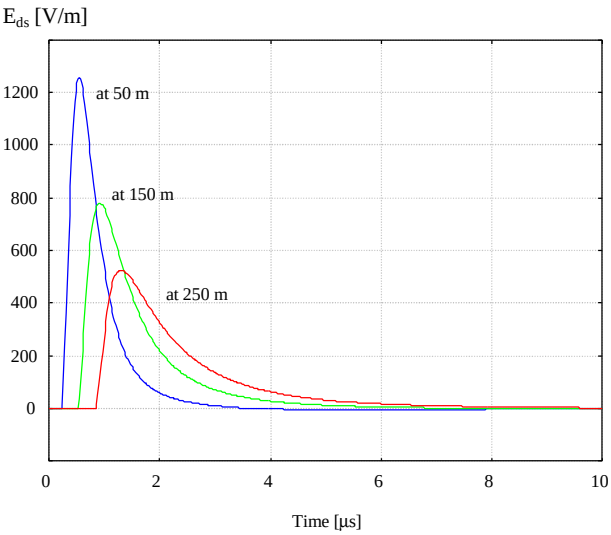

Figure 5 - Distributed voltage sources along the line, in the same system configuration considered for figures 3 and 4.

3. Corona modeling

It is assumed that the corona phenomenon may be completely accounted for by means of an appropriate, multivalued nonlinear function, the dynamic p. u. l. capacitance, C_{dyn}, defined as

$$C_{dyn}=\frac{dq}{dv} \qquad (7)$$

which represents the slope of the q-v characteristics and differs from the geometrical capacitance only when the voltage is increasing and its value is greater than a corona onset voltage, v_{co}, which is given by [15]:

$$v_{co} = E_c C_w C_p \left(1 + \frac{0.3}{\sqrt{r_w}}\right) r_w \frac{2h - r_w}{2h} \ln\left(\frac{2h - r_w}{r_w}\right) \quad (8)$$

where E_c = 30 kV·cm^{-1}, h and r_w are, respectively, the height and the radius of the conductor and C_w and C_p are coefficients taking into account the weather conditions and the polarity of the voltage.

Even though different formulation do exist [17], it is generally assumed [14-15] that, in case of multiconductor configurations, only diagonal terms are affected by corona, the mutual terms remaining the same as determined by the geometrical arrangement. It should be noted that corona losses derive directly from the q-v hysteretic corona behavior and no need of a distributed conductance or other equivalent circuits arises.

Many authors [1,13] adopted for the q-v characteristics a simplified linearized model or a very similar one [14]. However, the model proposed by Malik et al. [15], based on the evaluation of the conductor radius under corona conditions and on image theory, appears to be more general and less prone to the values of coefficients obtained experimentally, whose usability in configurations different from those used for their assessment is difficult to predict.
In particular, it appears interesting to compare the results obtained by means of the above methods. When adopting the Inoue method, it has been assumed for each diagonal term of the capacitance matrix the following expression:

$$C_{dyn} = \begin{cases} C_{geo} & \text{if } |v| < v_{co} \text{ or } \dfrac{\partial v}{\partial t} < 0 \\ C_{geo} + \dfrac{\alpha}{v}(v - v_{co})^{\beta} & \text{otherwise} \end{cases} \quad (9)$$

being $\alpha = (30 \div 45) \cdot 10^{-11} \cdot \sqrt{r_w / 2h}$ and $\beta \in [1,1.2]$.

In the Malik' model, it is assumed that a delay τ_c (in the order of 0.1 μs) exists before the conductor voltage yields to the corresponding corona charge; then, under corona conditions, it is assumed:

$$C_{dyn}(t) = C_{geo} + \frac{2\pi\varepsilon_0}{\Delta} + \frac{\pi\varepsilon_0}{\Delta - 1} \cdot \frac{h\left[r_w + \dfrac{v(t - \tau_c)}{0.9E_c}\right]\Delta - \left[r_w + \dfrac{v(t - \tau_c)}{0.9E_c}\right]^2}{h^2 \cdot \Delta^3} \quad (10)$$

where

$$\Delta = \frac{2h - r_c}{2h} \ln\left(\frac{2h - r_c}{r_c}\right) \quad (11a)$$

and the conductor radius after corona onset, r_c, is determined by solving, at each position along the line and at each time instant, the following nonlinear equation:

$$\left[r_w + \frac{v(t - \tau_c)}{0.9E_c}\right] = r_c(1 + \Delta) \quad (11b)$$

In Figure 6, a typical q-v diagram is reported, as obtained by means of the two simulation models; the considered line has an height of 10 meters and a radius of 1 cm, corresponding to a corona onset voltage of about 180 kV.

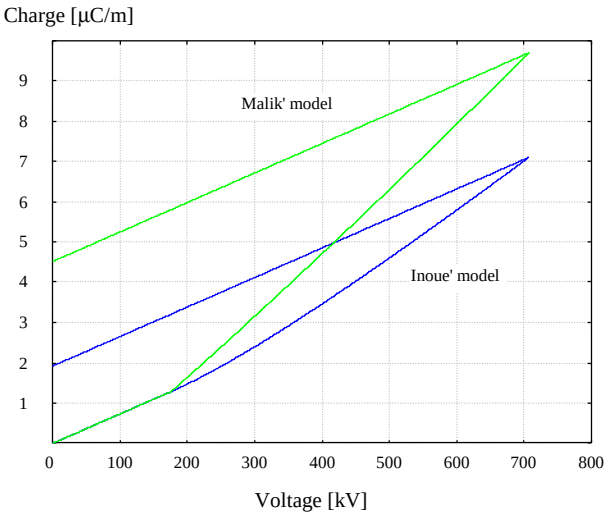

Figure 6 - Q-V characterisitcs as per Malik' [14] and Inoue' [13] model.

4. Terminal nonlinear loads

Each conductor is terminated at both ends on a parallel-connection between the load R_L and a Zn-O surge-arrester, as shown in figure 7, for the receiving end, at x=L.

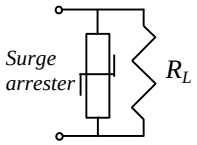

Figure 7 - Nonlinear load terminating each phase-conductor.

The Zn-O surge-arrester has been modelled by [16]:

$$i = k(v / v_{ref})^q = m \cdot v^q \quad (12)$$

with k = 2.5 kA, q = 24 and v_{ref} = 40 kV. The corresponding V-I characteristic is shown in figure 8.

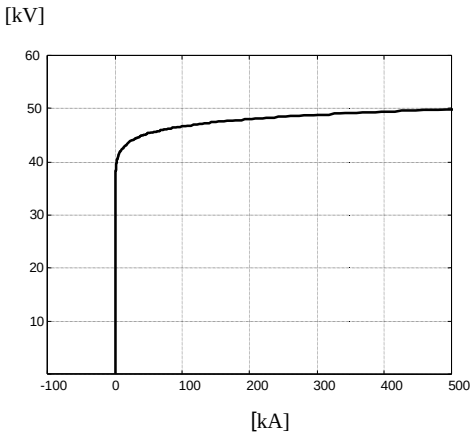

Figure 8 - V-I Characteristic of the Zn-O surge arrester.

5. Numerical solution algorithm

A numerical procedure based on the Finite Difference Time Method (FDTD) has been adopted for the solution of the MTL equations. As usual, positions and time instants for the calculation of voltages and currents are interlaced. Denoting matrices by bold characters, the time-marching nonlinear equations systems to be solved at the two ends of the lineat the time t = (n+1)·Δt are:

$$0.5\left(\mathbf{1}+\mathbf{R}_s\mathbf{C}_1\frac{\Delta x}{\Delta t}\right)\mathbf{V}_1^{n+1}+0.5\left(\mathbf{1}-\mathbf{R}_s\mathbf{C}_1\frac{\Delta x}{\Delta t}\right)\mathbf{V}_1^{n}+\mathbf{R}_s\frac{m}{2^q}\left(\mathbf{V}_1^{n+1}+\mathbf{V}_1^{n}\right)^q=\mathbf{E}_s^{n+1/2}+\mathbf{R}_s\mathbf{J}_{ds\_1}^{n+1/2}-\mathbf{R}_s\mathbf{I}_{1/2}^{n+1/2} \quad (13a)$$

$$0.5\left(\mathbf{1}+\mathbf{R}_L\mathbf{C}_L\frac{\Delta x}{\Delta t}\right)\mathbf{V}_L^{n+1}+0.5\left(\mathbf{1}-\mathbf{R}_L\mathbf{C}_L\frac{\Delta x}{\Delta t}\right)\mathbf{V}_L^{n}+\mathbf{R}_L\frac{m}{2^q}\left(\mathbf{V}_L^{n+1}+\mathbf{V}_L^{n}\right)^q=\mathbf{R}_L\mathbf{J}_{ds\_L}^{n+1/2}+\mathbf{R}_L\mathbf{I}_{L-1/2}^{n+1/2} \quad (13b)$$

where $\mathbf{C}_k$, k = 1, .. L, represents the capacitance matrix at the abscissa k·Δx, which because of corona may differ from the geometrical one.
Along the line, the voltage is obtained by solving the following linear equation system:

$$\mathbf{V}_k^{n+1}=\mathbf{V}_k^{n}+\mathbf{C}_k^{-1}\frac{\Delta t}{\Delta x}\left(\mathbf{J}_{ds\_k}^{n+1/2}+\mathbf{I}_{k-1/2}^{n+1/2}-\mathbf{I}_{k+1/2}^{n+1/2}\right) \quad (14)$$

It should be noted that the capacitance matrix at each time step and space position should be evaluated as function of the voltage at a time t-τ_c, which is known.

As to the current calculation, the following time-marching equation holds:

$$\mathbf{I}_{k+1/2}^{n+1/2}=\mathbf{I}_{k+1/2}^{n-1/2}+\mathbf{L}^{-1}\Delta t\left(\frac{\mathbf{V}_k^{n}-\mathbf{V}_{k-1}^{n}}{\Delta x}+\mathbf{E}_{ds\_k+1/2}^{n}\right) \quad (15)$$

5. Results and validation

The procedure and the models discussed have been applied to a 500-m-long MV three-phase line illuminated by a lightning stroke in close proximity of the left end of the line (x = - 250 m, r = 50 m). The parameters of the lightning return stroke current are those in Table I with an amplitude 5 times greater than that reported. The height of the line conductors is assumed to be 18 meters and wire radiii of 1 cm have been cosnidered. Distances between adjacent conductors are 1 meter.

In Fig. 9 the time trend of the induced voltage at the right end of the line is reported in case of linear terminal conditions and considering the two corona models. As expected the presence of corona will increase the value of the induced overvoltage. The line is terminated, at both the ends, on diagonal matrices of resistances, being R_{kk} = 500 Ω.

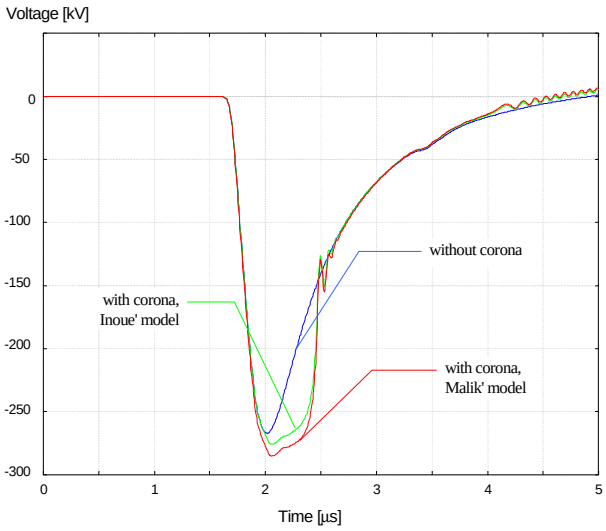

Figure 9 - Induced overvoltages in a three-phase line, modeling or not the corona phenomenon.

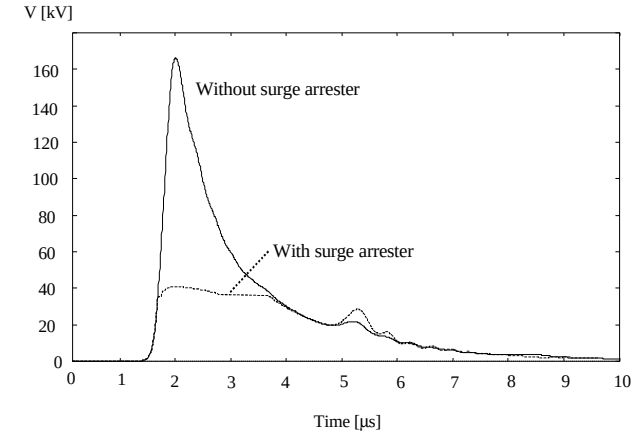

(a)

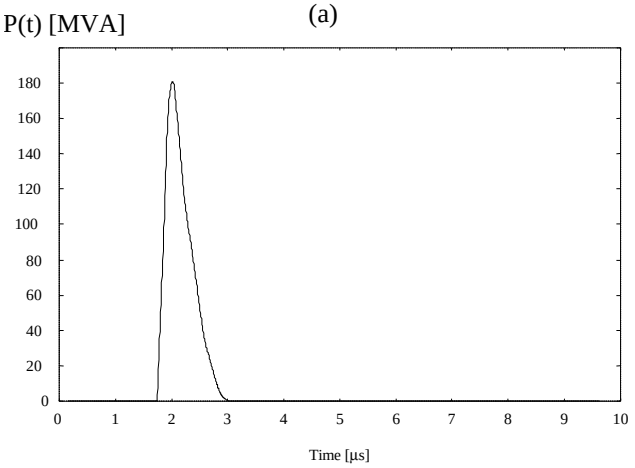

(b)

Figure 10 – Terminal voltage with and without the surge arresters (a) and instaneous power of the nonlinear protection device (b).

In figures 10 the time trends of the terminal voltage with and without the nonlinear load (a) and that of the power involving the surge arrester (b) are reported; the line configuration is similar to that already described, but a line height of 12 meters has been considered. The characteristic of the nonlinear loads, which are connected only at the right end of the line, is that shown in figure 8.

6. Conclusions

The prediction of indirect lightning – induced overvoltages in multiconductor transmission lines has been presented. The effects of possible onset of the corona phenomenon have been accounted for, as well as the presence of nonlinear loads like metal-oxide varistors.

References

[1] C. Gary, A. Timotin, D. Cristescu, "Prediction of surge propagation influenced by corona and skin effect", *IEE Proc. - Pt. A*, 1983, pp. 264-272.

[2] C. A. Nucci, F. Rachidi, M. Ianoz, C. Mazzetti, "Lightning-induced voltages on overhead power lines", *IEEE Trans. on EMC*, 1993, pp.75-86.

[3] M. J. Master, M. A. Uman, "Lightning induced voltages on power lines: theory", *IEEE Trans. on PAS*, 1984, pp. 2502-2518.

[4] F. Heidler, "Analytische Blitzstromfunktion zur LEMP- Berechnung", (in German), *Proc. 18th Int. Conf. Lightning Protection*, Munich, 1985.

[5] V. A. Rakov, M. A. Uman, "Review and evaluation of lightning return stroke models including some aspects of their application", *IEEE Trans. on EMC*, 1998, pp. 403-426.

[6] C. A. Nucci, C. Mazzetti, F. Rachidi, M. Ianoz, "On lightning return stroke models for LEMP calculations", *Proc. 19th Int. Conf. Lightning Protection*, pp. 463-470, Graz, 1988.

[7] V. Cooray, V. Scuka, "Lightning-induced overvoltages in power lines: validity of various approximations made in overvoltages calculations", *IEEE Trans. on EMC*, 1998, pp. 355-363.

[8] H. K. Hoidalen, J. Sletbak, T. Enriksen, "Ground effects on induced voltages from nearby lightning", *IEEE Trans. on EMC*, 1997, pp. 269-278.

[9] C. D. Taylor, R. S. Satterwhite, C. W. Harrison, "The response of a terminated two-wire transmission line excited by a nonuniform electromagnetic field", *IEEE Trans. on Antennas Propagat.*, 1965, pp. 987-989.

[10] C. A. Nucci, F. Rachidi, "On the contribution of the electromagnetic field components in field-to-transmission line interaction", *IEEE Trans. on EMC*, 1995, pp. 505-508.

[11] F. Rachidi, C. A. Nucci, M. Ianoz, C. Mazzetti, "Influence of a lossy ground on lightning induced voltages on overhead lines" *IEEE Trans. on EMC*, 1996, pp. 250-264.

[12] M. A. Uman, D. K. McLain, E. P. Krider, "The electromagnetic radiation from a finite antenna", *American Journal of Physics*, 1975, pp. 33-38.

[13] C. A. Nucci, S. Guerrieri, M. T. Correia de Barros, F. Rachidi, "Influence of corona on lightning-induced voltages on overhead power lines", *Proc. of Int. Conf. on Power Systems Transients*, Lisbon, Portugal, 1995, pp. 306-311.

[14] A. Inoue, "Propagation analysis of overvoltage surges with corona based upon charge versus voltage curve", *IEEE Trans. on PAS*, 1985, pp. 655-660.

[15] Xiao-rong Li, O. P. Malik, Zhi-da Zhao, "A practical model of corona for calculation of transients on transmission lines", *IEEE Trans. on PWRD*, 1989, pp. 1145-1151.

[16] IEEE Working Group 3.4.11, "Modeling of MO surge arresters", *IEEE Trans. on PWRD*, 1991, pp. 302-309.

[17] M. T. Correia de Barros, "Identification of the capacitance coefficients of multiphase transmission lines exhibiting corona under transient conditions", *IEEE Trans. on PWRD*, 1995, pp. 1642-1648.